Synthesis, X-ray crystal structures, and computational studies of 1,1′-bridged 4,4′-diaryl-2,2′-bibenzimidazoles: building blocks for supramolecular structures†

Derik K. Frantz, Ashley A. Sullivan, Yoshizumi Yasui,‡ Anthony Linden, Kim K. Baldridge* and Jay S. Siegel*

Received 18th November 2008, Accepted 9th February 2009
First published as an Advance Article on the web 30th March 2009
DOI: 10.1039/b820502g

A series of C-shaped, 1,1′-alkyl-bridged 4,4′-diaryl-2,2′-bibenzimidazoles has been synthesized. The crystal structures of these compounds have been determined and packing diagrams demonstrate that these molecules either form linear intercalated molecular chains or include solvent molecules in the solid state. Crystal structures are compared to computational structures determined using density functional theory, with the BMK/DZV(2d,p) method. The C-shaped or tweezer-like geometry enables them to act as building blocks for supramolecular architectures.

Introduction

Synthetic access to supramolecular building blocks with discrete molecular geometries[1] enables the design of molecular machines[2] and devices.[3] To achieve this goal, such systems regularly incorporate multidentate ligands and metal complexes, which often exhibit additional useful coordination, photophysical, and electrochemical properties.[4] Bipyridine (bpy)[5] and phenanthroline (phen)[6] derivatives play a dominant role in this field, owing to their ready availability. A consequence of the use of bpy and phen is the construction of molecular geometries with multiples of 60° between bonding vectors (Fig. 1). In contrast, a 6,5 ring fusion presents a 90° relationship between positions 2 and 4, and coupling of the 2-positions results in a dimer with a 0° (*syn*) or 180° (*anti*) relationship between 4,4′ vectors. Heterocycles like 4,4′-disubstituted-2,2′-bibenzimidazole (BBI) represent such a class of ligands and can be easily prepared.[7]

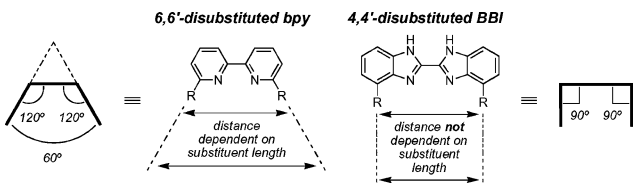

Fig. 1 Structural comparison of 4,4′-disubstituted BBI and 6,6′-disubstituted bpy.

In the present work we show that *N*,*N*′-bridged derivatives of 4,4′-disubstituted-BBI form a versatile class of organic molecular clips with tunable pitch and tweezer geometry. Molecular clips (and tweezers) have garnered much attention due to their ability to complex substates *via* noncovalent interactions. Seminal work in this field includes examples in which chemical pincers are connected by one bond to rotatable spacers[8] or flexible, heteroaromatic scaffolds.[9] Other examples incorporate aromatic pincers that are connected to spacers by two bonds at their *ortho* positions.[10] *N*,*N*′-Bridged derivatives of 4,4′-diaryl-BBI resemble molecular tweezers comprising dibenz[*c*,*h*]acridine, which were synthesized and investigated by Zimmerman and coworkers.[9] The distance between C(2) and C(12) of dibenz[*c*,*h*]acridine is 7.2 Å, allowing the tweezers to complex many aromatic substrates.[9b] The distance between pincers connected to the 4- and 4′-positions of a BBI-based spacer could vary, depending on the length and type of the group bridging the 1- and 1′-positions. This distance would be expected to be ~8 Å in a flat BBI spacer, which is within the range expected to complex aromatic substrates.

The parent BBI complexes transition metals in a variety of binding modes[11] and states of deprotonation, formally neutral,[12–14] monoanionic,[15] and dianionic states.[16–18] Often used as a bridging ligand, BBI can participate in mono-, di-, tri-, and tetrametallic complexes.[11] BBI derivatives have appeared recently in general supramolecular applications,[19] as well as in the formation of a molecular switch[20] and in photophysical energy transfer complexes.[21] The N–H groups at the 1,1′-positions act as hydrogen bond donors to carboxylate anions, and several BBI–carboxylate complexes have been developed.[22] Hydrogen bonding has also been observed between the 1,1′-positions of BBI and a metal nitrile complex.[23] Therefore, BBI building blocks embody functional and geometrical features of importance for supramolecular architectures.

Synthesis[24]

We have recently reported the synthesis of Boc-protected 4,4′-diaryl-BBI derivatives[7] of type **1** *via* Negishi[25] cross-coupling reactions. These fluorescent compounds exist primarily in the *anti* (Z-shaped) conformation.[26]

Institute of Organic Chemistry, University of Zurich, Winterthurerstrasse 190, CH-8057, Zurich, Switzerland. E-mail: jss@oci.uzh.ch; Fax: +41 (0)44 635 6888; Tel: +41 (0)44 635 4281

† Electronic supplementary information (ESI) available: Experimental information. CCDC reference numbers 710114–710119. For ESI and crystallographic data in CIF or other electronic format see DOI: 10.1039/b820502g

‡ Current address: WPI Advanced Institute for Materials Research, Tohoku University, Japan.

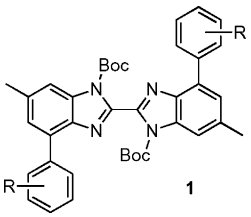

Connecting the 1,1′-positions with small bridges forces the BBI structure to adopt a C-shaped conformation suitable for a variety of more complex structures (Fig. 2). Examples of such structures are tetrahedral complexes of BBI derivatives with two small monodentate ligands (A), one bidentate ligand (B), or another BBI derivative (C). Macrocyclic ligands (D) and molecular rectangles (E) could also be generated from BBI-based building blocks. Additional supramolecular utility arises from the distance between the 4,4′-aryl groups (~8 Å), which nears the ideal van der Waals distance for inclusion of an aryl group by a tweezer system.

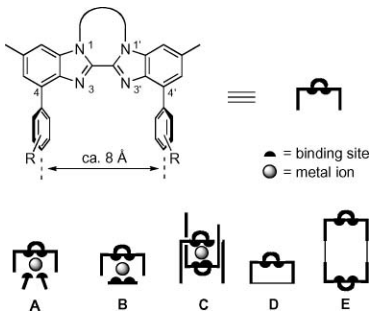

Fig. 2 Examples of higher order structures that could include the 1,1′-bridged 4,4-diaryl-BBI structural motif.

Bridging of the 1,1′-positions could be accomplished by several means: 1) alkyl bridges could serve as strong, covalently bonded tethers that would completely impede rotation about the inter-annular 2,2′-C–C bond;[27] 2) hydrogen-bonded bridges[20,21] at the 1,1′-positions could induce a structural change in BBI, leading to the *syn* conformer; 3) inorganic bridges could be generated by introduction of bulky metal complexes[28] that selectively bind to the *exo* binding sites.

Focusing on method 1, six bridged BBI derivatives (**3a–f**), which differ in the type and length of their bridge and the conformational preferences of their 4,4′-aryl substituents, were targeted for synthesis and structural study (X-ray and DFT computations[29]). Bridges were limited to *o*-xylylene (**3a–b**), trimethylene (**3c–d**), and dimethylene (**3e–f**) and aryl substituents at the 4,4′-positions were limited to 4-methoxyphenyl (**3a**,**c**,**e**) and 4-methoxy-2,6-dimethylphenyl groups (**3b**,**d**,**f**).[30] The length of the bridge was expected to control the torsion angle about the 2,2′-C–C bond, as larger bridges were expected to lead to more twisted – and more flexible – ground-state structures. The two types of 4,4′-aryl substituents differ in their conformational preference against the BBI framework; the 4-methoxyphenyl groups prefer skewed-close-to-conjugated geometries and have relatively free rotation profiles,[31] whereas the 4-methoxy-2,6-dimethylphenyl groups, which bear sterically bulky flanking methyl groups, prefer a skewed-close-to-orthogonal conformation and have a hindered rotational profile.

The synthesis of a generic, bridged BBI **3** can be accomplished by either deprotecting **1** and treating BBI derivative **2** with an alkyl dihalide or by coupling aryl groups to a bridged dihalide (Scheme 1). It was found that the first approach yielded good results and the second approach was unsuccessful, likely because poor solubility of the bridged dibromides **5** hindered their ability to partake in coupling reactions. Synthesis of **3a–f** was accomplished by treating **2a** and **2b** with alkyl dihalides in the presence of Cs_2CO_3 and NaI in THF (Scheme 2).

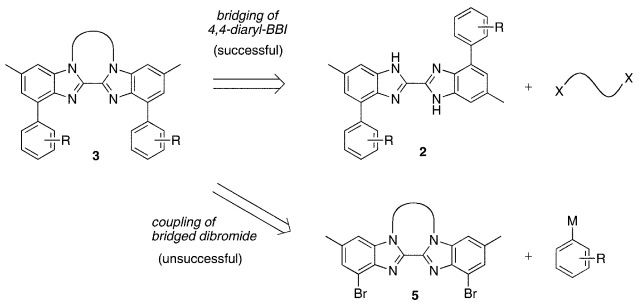

Scheme 1 The two attempted synthetic routes to bridged BBI **3**.

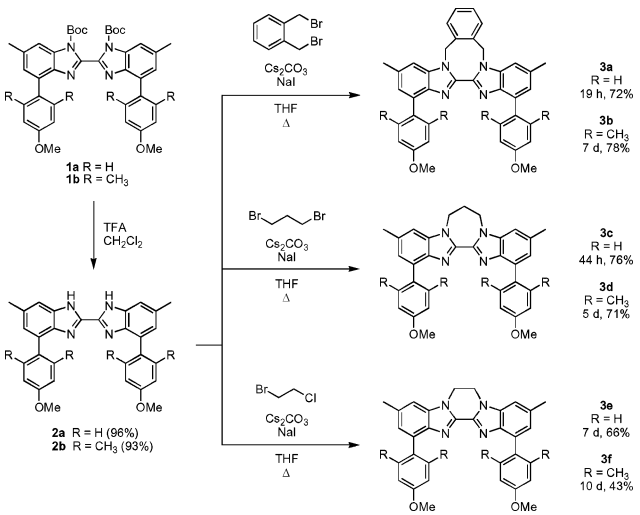

Scheme 2 Synthesis of 1,1′-bridged 4,4′-diaryl-BBI.

The generation of **3a–f** by alkylation of **2a–b** in THF often requires long reaction times. Recently, we discovered that the dibromides **5a–c** could be prepared from 4,4′-dibromo-6,6′-dimethyl-BBI[7] (**4**) by analogous alkylation using K_2CO_3 in DMF at shorter reaction times and with good yields (Scheme 3). Preliminary investigation of the DMF conditions for the formation of **3** from **2** is promising. Further work to elaborate these results is ongoing.

Structure

Structural parameters of relevance to this study include the torsion angles about the α- (purple and blue) and ϕ-axes (green) and the distance between the centroids of the 4- and 4′-aryl groups (Fig. 3). The α_{BBI} torsion angle is defined as the dihedral angle between the two planar bibenzimidazole moieties.[32] The α_{bridge} torsion angle is defined as the twist about the 2,2′ C–C axis of the first carbon atom on each side of the bridge. The α_{aryl} torsion angle is defined as the twist about the 2,2′ C–C axis of the centroids of the 4- and 4′-aryl groups. The ϕ torsion angle is defined as the dihedral angle

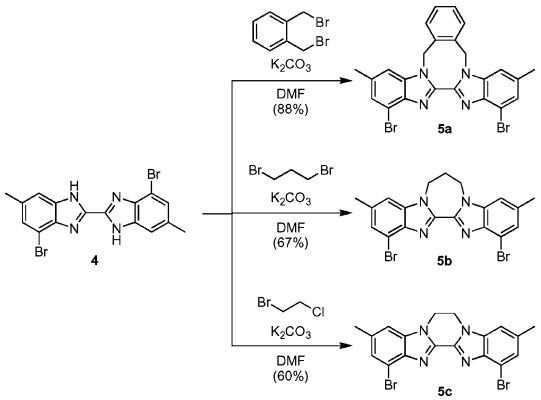

Scheme 3 Synthesis of bridged dibromides **5a–c**.

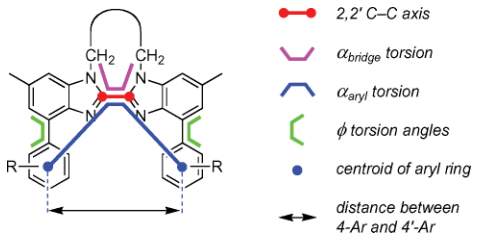

Fig. 3 Diagram of measurements used in the discussion of the structural properties of bridged BBI.

between the planes of the rings at the 4- and 4′-positions and the planes of the benzimidazole moieties connected to them.[33]

Structural data for **3a–f** was collected from X-ray crystallographic and computational studies (Table 1).[34] Computational BMK/DZV(2d,p) structures of **3a–f** were determined in symmetries C_2 and/or C_s. Frequency analysis confirmed each structure to be a minimum on the potential energy surface. These structures are taken as ideal structures for the molecule in isolation. Two general trends can be seen among the C_2-symmetric structures: 1) bridge length correlates to α torsion angle; 2) *ortho*-substitution on the 4-aryl group increases ϕ (Fig. 4).

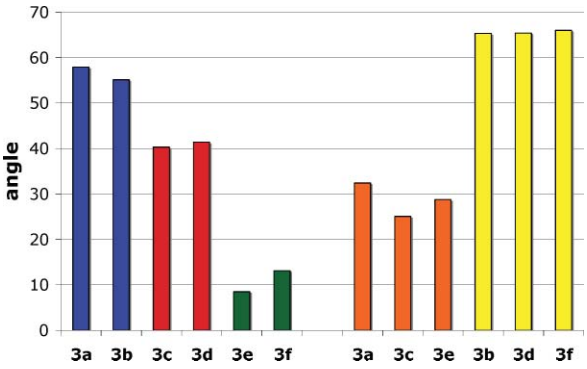

Fig. 4 Trend in α_{BBI} torsion vs. bridge length (left); trend in ϕ torsion vs. *ortho*-aryl substitution (right) – computational data of C_2 structures.

In the case of the trimethylene bridge, a C_s isomer was considered and found to be of comparable energy to the C_2 conformer. In all other cases, the C_2 form was predicted to dominate. The twisted, C_2-symmetry-optimized structures were calculated to have lower energies than their respective C_s structures by 1.4 kcal/mol (**3c**) and 2.4 kcal/mol (**3d**). The 7-membered rings in **3c** and **3d**, which arise from bridging the 1,1′-positions with a 3-atom bridge, can adopt an envelope or a twisted conformation, leading to C_s- or C_2-symmetric structures, respectively. By definition, the optimized C_s-symmetric structures must have α torsion angles equal to zero. A further structural ramification of the C_s conformer is to effectively "shorten" the aryl-centroid distance by *ca.* 1.5 Å. No significant effect on ϕ was seen in the C_s conformers compared to the C_2 conformers.

Crystals of **3a–f**, suitable for X-ray crystallographic analysis, were obtained from several solvent systems. **3a**, **3c**, and **3d** crystallized from either a solvent-layered or slowly evaporating mixture of CH_2Cl_2 and hexane. Compound **3b** crystallized from a slowly evaporating mixture of CH_2Cl_2 and acetone. The poorly soluble **3e** crystallized upon cooling a hot solution in DMF. Layering ether above an NMR sample in $CDCl_3$ yielded crystals of **3f** upon slow

Table 1 Selected geometric parameters of 1,1′-bridged-BBI compounds **3a–f**, as determined from the crystal structures and BMK/DZV(2d,p) calculations. Experimental values from crystal structures are given in plain text; calculated values are in *italics* together with their molecular symmetry

	α_{BBI} torsion (°)	α_{bridge} torsion (°)	α_{aryl} torsion (°)	ϕ torsion (°)	4,4′-aryl distance (Å)
3a	38.8(1)	58.1(1)	32.2(2)	27.7(3), 37.8(3)	8.586(2)
3a (C_2)	*57.9*[c]	*64.6*	*66.8*	*32.4*	*9.88*
3b	58.4(1)[c]	64.2(1)	65.1(2)	71.6(1), 81.7(1)	9.782(3)
3b (C_2)	*55.1*[c]	*63.8*	*60.5*	*65.3*	*9.52*
3c	22.8(1)	19.7(2)	23.3(2)	36.4(1), 44.9(1)	8.382(4)
3c (C_s)	*0*	*0*	*0*	*25.1*	*7.71*
3c (C_2)	*40.3*	*47.3*	*43.5*	*32.7*	*9.20*
3d	16.6(1)	12.1(1)	13.0(1)	70.2(1), 71.0(1)	7.655(3)
3d (C_s)	*0*	*0*	*0*	*65.4*	*7.51*
3d (C_2)	*41.4*	*47.5*	*43.1*	*65.7*	*9.01*
3e[a] (A)	15.6(1)	18.2(1)	2.6(2)	48.7(1)[b]	8.595(4)
3e[a] (B)	15.1(1)	17.3(1)	12.5(2)	30.3(1)[b]	9.145(3)
3e (C_2)	*10.5*	*16.7*	*10.2*	*28.8*	*8.99*
3f	5.5(1)	14.1(2)	5.1(4)	67.1(2), 68.4(2)	8.193(7)
3f (C_2)	*13.1*	*17.5*	*15.3*	*66.0*	*8.93*
5a	55.5(2)	62.9(2)	64.4(7)[d]	—	—

[a] Compound **3e** crystallized with two symmetry-independent molecules (A and B) in the unit cell. [b] The molecules have crystallographic C_2-symmetry, giving equal values of ϕ for both aryl groups. [c] The literature value of 63.9° for α_{BBI} in the crystal structure of 1,1′:3,3′-*o*-xylylene-dibridged BBI is slightly higher than this range.[35] [d] The α_{aryl} torsion angle of **5a** involved the pendant bromine atoms instead of ring centroids.

mixing of the solvents. Dibromide **5a** crystallized from a slowly evaporating CH_2Cl_2–ethyl acetate solvent mixture.

In addition to the calculated structures, the α torsion angles of the molecular structures of *o*-xylylene-bridged compounds **3a** and **3b** (Fig. 5) can be compared to the molecular structure of bridged dibromide **5a**. The α torsion angles in **5a**, which has crystallograpically-imposed twofold symmetry, are similar to those found in the calculated structures of **3a** and **3b**.

Fig. 5 (left) Experimental structure[36] of **3a**. (right) Experimental structure of **3b**, with the molecule of acetone removed for clarity.

The crystal structure of **3a** exhibits tongue-in-groove stacking (Fig. 6) with the xylylene moiety of one molecule filling the cavity between the 4- and 4′-aryl groups of a neighboring molecule. In contrast, the crystal structure of **3b** is an acetone solvate with the molecule of acetone situated beside the 4,4′ aryl groups. Each molecule–solvent complex is a discrete entity within the lattice. This difference shows up in the molecular geometry as compared to the computational ideal. The experimental structure of **3b** exhibits α_{BBI}, α_{bridge}, and α_{aryl} torsion angles that are similar to the calculated values. Its ϕ torsion angles are higher than the calculated values, which is likely due to crystal packing in accommodating the solvent molecule. In contrast to **3b**, the experimental structure of **3a** deviates significantly from its optimized gas-phase structure. The packing in linear molecular arrays, which stack tightly and extend in alternating, opposite directions, leads to a reduction of the α_{BBI} and α_{aryl} torsion angles. The experimental structure of **3a** exhibits α_{BBI} and α_{aryl} torsion angles that are more than 19° and 34° lower than the calculated values, respectively. This increase in planarity also causes the 4,4′-aryl distance to be shorter in the crystal structure than in the optimized gas-phase structure by nearly 1.3 Å. The disparity between the α_{bridge} and the other α torsion angles primarily arises from non-planarity of the 1,1′-nitrogen atom centers, which show some sp^3 character.

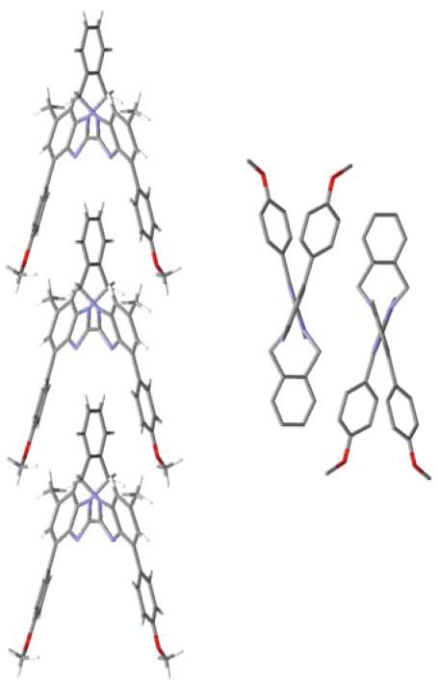

Fig. 6 (right) Packing of **3a**, showing linear, tongue-in-groove stacking. (left) Face-to-face packing of molecules of **3a** (hydrogen atoms removed for clarity).

The π-interactions between the neighboring aromatic groups within the tongue-and-groove arrangement is not ideal nor symmetric; the aryl planes form a *ca.* 14° or 26° angle with the plane of the neighboring xylyl ring along the stack. The former being close to parallel and having a 3.7 Å plane-to-centroid distance is indicative of a face-to-face center-to-edge geometry. The distances between the centroid-to-centroid distances of the xylylene and neighboring aryl rings are 4.36 Å and 4.74 Å, respectively. In contrast, the angle between aryl rings of adjacent stacks is prescribed by the unit cell symmetry to be parallel, the distance centroid-to-plane being ca. 3.6 Å, essentially an ideal face-to-face, center-to-edge geometry. Overall, it would seem that molecules of **3a** "bind" their neighbor in the crystal and clamp down to optimize the interactions.

The crystal structures of **3c** and **3d** contain solvent molecules (CH_2Cl_2) in the cavities between their 4- and 4′-aryl arms (Fig. 7). There is one molecule of CH_2Cl_2 per molecule of **3c** and two molecules of CH_2Cl_2 per molecule of **3d** in their respective crystal structures. The included solvent molecule(s) may cause the experimental structure of **3c** and **3d** to have larger ϕ torsion angles than their computational structures. The molecules in both crystal structures exhibit α torsion angles that are smaller than their optimized C_2 structures. The α torsion angles and

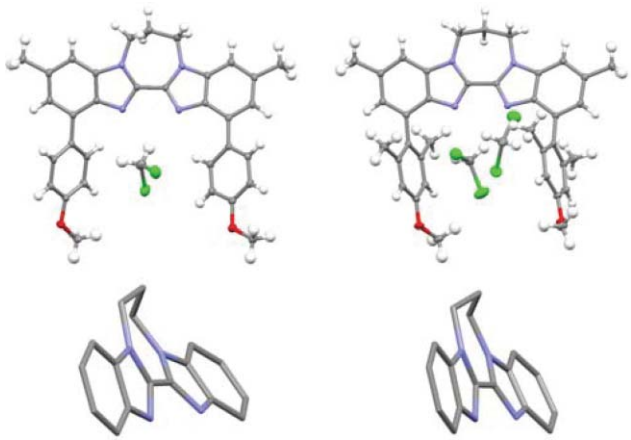

Fig. 7 (top left) Experimental structure of **3c**, containing one molecule of CH_2Cl_2 in its cavity. (top right) Experimental structure of **3d**, containing two molecules of CH_2Cl_2. (bottom left) 1,1′-Trimethylene-bridged-BBI moiety of **3c**, showing some puckering of the central atom of the bridge. (bottom right) Same view of **3d**, showing significant puckering of the central atom of the bridge.

the 4,4′-aryl distance in the experimental structure of **3c** indicate a structure that lies roughly halfway between the C_s and C_2 optimized structures. The solid state molecular geometry of **3d** also appears to lie between the computational C_s and C_2 structures, but resembles the optimized C_s structure more closely. Its α torsion angles are small and its 4,4′-aryl distance is much closer to that of the optimized C_s structure than that of the optimized C_2 structure.

The dimethylene-bridged compounds, **3e** and **3f** (Fig. 8), participate in tongue-in-groove stacking (Fig. 9) similar to that observed in the crystal structure of **3a**. Unlike the crystal structure of **3a**, neighboring molecules of **3e** and **3f** lie in alternating planes. Compound **3e** crystallized with two symmetry-independent molecules (A and B) in the unit cell, each with crystallographic C_2 symmetry. In the tongue-in-groove stacking, the arms of a molecule (A) grips the head of a molecule (B), and this continues to give an ABAB pattern. The computational structure of **3e** shows an α_{bridge} torsion angle that is higher than both the α_{BBI} and the α_{aryl} torsion angles, due to slight non-planarity of the 1,1′-nitrogen atom centers. This trend is observed to a lesser extent in the experimental structure, both in molecule (A) and in molecule (B). The experimental structure of molecule (A) deviates to some extent from the calculated structure in the α_{aryl} torsion angle and the 4,4′-aryl distance, which are correlated. The ϕ torsion angle is much higher in the experimental structure of molecule (A) than in its computational structure or the experimental structure of molecule (B). This increase in torsion angle is caused by the inclusion of part of molecule (B). Compound **3f** also participates in tongue-in-groove stacking, but all of the molecules are symmetry-dependent. Values of the α_{BBI} and α_{aryl} torsion angles, are somewhat lower in the experimental structure than in the computational structure. The torsion angle[37] between the BBI moieties of neighboring molecules is 83° for **3e** and 57° for **3f**.

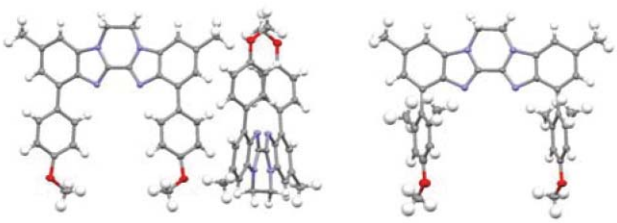

Fig. 8 Experimental structures of **3e** (left) and **3f** (right).

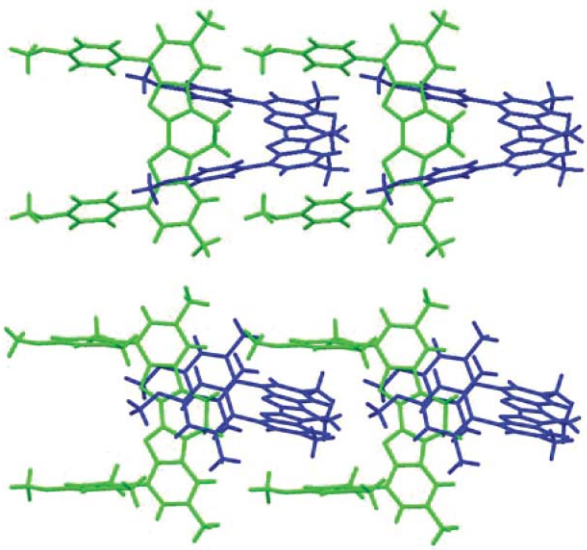

Fig. 9 Linear crystal stacking arrays of wedged ethylene-bridged **3e** (top) and **3f** (bottom).

Conclusions

In this investigation, 1,1′-bridged derivatives of 4,4′-diaryl-BBI were synthesized and their crystal structures examined and compared to BMK/DZV(2d,p) calculated structures. Bridged dibromides **5a–c** were also prepared, and the crystal structure of **5a** was obtained. The crystal structures and DFT structures of **3a–f** usually closely agree, except when crystal packing causes significant changes in molecular structure. The most noticeable example of such a structural change was observed for **3a**. These BBI derivatives, which resemble clips, show a propensity to include other molecules between their 4,4′-aryl arms. Compounds **3a**, **3e** and **3f** crystallize with aromatic systems of neighboring molecules within this cavity. Compounds **3b**, **3c** and **3d** crystallize as solvates and the molecules of solvent are located between the aryl groups in **3c** and **3d**. With an understanding of the structures of compounds **3a–3f**, future work on the supramolecular applications of these systems can be investigated.

Experimental[24]

Computational methods

The conformational analyses of the molecular systems described in this study, including structural parameters, orbital arrangements, and properties, were carried out using the Gaussian98[38] and GAMESS[39] software packages. The density functional method using the BMK functional,[40] was used together with Dunning's double-polarized basis set DZ(2d,p).[41] Full geometry optimizations were performed and uniquely characterized *via* second derivatives (Hessian) analysis to determine the number of imaginary frequencies (0 = minima; 1 = transition state). Molecular orbital contour plots, used as an aid in the analysis of results, were generated and depicted using the program QMView.[42]

Acknowledgements

We thank the Swiss National Science Foundation for support of this work. We acknowledge Severin Schneebeli for some preliminary computational studies on **3e** and **3f**. YY would like to thank the Legerlotz Fund of the Organic Chemistry Institute of the University of Zurich.

References and notes

1 J.-M. Lehn, *Supramolecular Chemistry: Concepts and Perspectives*, VCH, Weinheim, Germany, 1995.
2 V. Balzani, A. Credi, F. M. Raymo and J. F. Stoddart, *Angew. Chem. Int. Ed.*, 2000, **39**, 3348.
3 (*a*) A. P. de Silva, H. Q. N. Gunaratne, T. Gunnlaugsson, A. J. M. Huxley, C. P. McCoy, J. T. Rademacher and T. E. Rice, *Chem Rev.*, 1997, **97**, 1515; (*b*) T. W. Bell and N. M. Hext, *Chem Soc. Rev.*, 2004, **33**, 589.
4 V. Balzani, A. Juris, M. Venturi, S. Campagna and S. Serroni, *Chem Rev.*, 1996, **96**, 759.

5 G. R. Newkome, A. K. Patri, E. Holder and U. S. Schubert, *Eur. J. Org. Chem.*, 2004, 235.
6 P. G. Sammes and G. Yahioglu, *Chem. Soc. Rev.*, 1994, **23**, 327.
7 Y. Yasui, D. K. Frantz and J. S. Siegel, *Org. Lett.*, 2006, **8**, 4989.
8 C.-W. Chen and H. W. Whitlock, *J. Am. Chem. Soc.*, 1978, **100**, 4921.
9 (*a*) S. C. Zimmerman and C. M. VanZyl, *J. Am. Chem. Soc.*, 1987, **109**, 7894; (*b*) S. C. Zimmerman and K. W. Saionz, *J. Am. Chem. Soc.*, 1995, **117**, 1175.
10 (*a*) A. E. Rowan, J. A. A. W. Elemans and R. J. M. Nolte, *Acc. Chem. Res.*, 1999, **32**, 995; (*b*) F.-G. Klärner and B. Kahlert, *Acc. Chem. Res.*, 2003, **36**, 919.
11 R. Usón, L. A. Oro, J. Gimeno, M. A. Ciriano, J. A. Cabeza, A. Tiripicchio and M. T. Camellini, *J. Chem. Soc. Dalton Trans.*, 1983, 323.
12 For BBI complexes with metals in group 8, see: (*a*) D. Boinnard, P. Cassoux, V. Petrouleas, J.-M. Savariault and J.-P. Tuchagues, *Inorg. Chem.*, 1990, **29**, 4114; (*b*) M. Haga, *Inorg. Chem. Acta*, 1983, **75**, 29; (*c*) M. Haga and A. M. Bond, *Inorg. Chem.*, 1986, **25**, 4507; (*d*) S. Rau, B. Schäfer, A. Grüßing, S. Schebesta, K. Lamm, J. Vieth, H. Görls, D. Walther, M. Rudolph, U. W. Grummt and E. Birkner, *Inorg. Chem. Acta*, 2004, **357**, 4496.
13 For BBI complexes with metals in group 10, see: (*a*) A. C. Dash, A. N. Acharya and R. Sahoo, *Transition Met. Chem.*, 1996, **21**, 337; (*b*) R. Usón, J. Gimeno, L. A. Oro, M. A. Aznar and J. A. Cabeza, *Polyhedron*, 1983, **2**, 163.
14 For BBI complexes with metals in group 11, see: (*a*) S. S. Lemos, V. M. Deflon, K. E. Bessler, M. P. Abbott and E. Niquet, *Transition Met. Chem.*, 2004, **29**, 46; (*b*) R. Usón, J. Vicente and M. T. Chicote, *J. Organomet. Chem.*, 1981, **209**, 271.
15 (*a*) M. P. Gamasa, E. Garcia, J. Gimeno and C. Ballesteros, *J. Organomet. Chem.*, 1986, **307**, 39; (*b*) J. R. Galán-Mascarós and K. R. Dunbar, *Angew. Chem. Int. Ed.*, 2003, **42**, 2289. See refs. 12c and 11.
16 For BBI–Ti complexes, see: B. F. Fieselmann, D. N. Hendrickson and G. D. Stucky, *Inorg. Chem.*, 1978, **17**, 2078.
17 For BBI complexes with metals of groups 7 and 8, see: (*a*) P. H. Dinolfo, K. D. Benkstein, C. L. Stern and J. T. Hupp, *Inorg. Chem.*, 2005, **44**, 8707; (*b*) M. Haga and A. M. Bond, *Inorg. Chem.*, 1991, **30**, 475; (*c*) M. Haga, T. Matsumura-Inoue and S. Yamabe, *Inorg. Chem.*, 1987, **26**, 4148. See refs. 12b,c.
18 For BBI complexes with metals of groups 9, 10 and 11, see: (*a*) D. Carmona, J. Ferrer, A. Mendoza, F. J. Lahoz, L. A. Oro, F. Viguri and J. Reyes, *Organometallics*, 1995, **14**, 2066; (*b*) R. Usón and J. Gimeno, *J. Organomet. Chem.*, 1981, **220**, 173; (*c*) R. Usón, J. Gimeno, J. Forniés and F. Martínez, *Inorg. Chem. Acta*, 1981, **50**, 173; (*d*) M. S. Haddad and D. N. Hendrickson, *Inorg, Chem.*, 1978, **17**, 2622; (*e*) R. Usón, J. Vicente and M. T. Chicote, *J. Organomet. Chem.*, 1981, **209**, 271; (*f*) B.-C. Tzeng, D. Li, S.-M. Peng and C.-M. Che, *J. Chem. Soc. Dalton Trans.*, 1993, 2365. See refs. 11, 13b and 14a.
19 S. Rau, M. Ruben, T. Büttner, C. Temme, S. Dautz, H. Görls, M. Rudolph, D. Walther, M. Duati, S. Fanni and J. G. Vos, *J. Chem. Soc. Dalton Trans.*, 2000, 3649.
20 S. Rau, T. Büttner, C. Temme, M. Ruben, H. Görls, D. Walther, M. Duati, S. Fanni and J. G. Vos, *Inorg. Chem.*, 2000, **39**, 1621.
21 S. Rau, B. Schäfer, S. Schebesta, A. Grüßing, W. Poppitz, D. Walther, M. Duati, W. R. Browne and J. G. Vos, *Eur J. Inorg. Chem.*, 2003, 1503.
22 S. Rau, L. Böttcher, S. Schebesta, M. Stollenz, S. Görls and D. Walther, *Eur. J. Inorg. Chem.*, 2002, 2800.
23 K. Halbauer, A. Göbel, A. Sterzik, H. Görls, S. Rau and W. Imhof, *Eur. J. Inorg. Chem.*, 2007, 1508.
24 At the request of the editor, synthetic and crystal structure experimental details have been moved to the ESI†.
25 E. Negishi, 'Overview of the Negishi Protocol with Zn, Al, Zr, and Related Metals', in *Handbook of Organopalladium Chemistry for Organic Synthesis*, ed. E. Negishi, Wiley & Sons, New York, 2002, Vol. 1, pp. 229–247.
26 The molecular structure of 1,1′-bis(*tert*-butoxycarbonyl)-4,4′-dibromo-6,6′-dimethyl-BBI shows an *anti* conformation.
27 (*a*) V. Goulle and R. P. Thummel, *Inorg. Chem.*, 1990, **29**, 1767; (*b*) Z. Shi and R. P. Thummel, *J. Org. Chem.*, 1995, **60**, 5935.
28 Refs. 11–18.
29 Optimized structures for 1,1′-bridged biindoles using early low-level calculations have been reported in ref. 27a.
30 For information about the synthesis of 1,1′-bridged BBI and 1,1′;3,3′-dibridged 2,2′-bibenzimidazolium salts, see ref. 27b and R. P. Thummel, V. Goulle and B. Chen, *J. Org. Chem.*, 1989, **54**, 3057.
31 Although it is true that the 4-$MeOC_6H_5$-group does not exhibit true "free" rotation ($\Delta G^{\ddagger}_{rot} = 0$), the rotational barrier could be expected to be quite low, allowing for fast rotation at room temperature.
32 The α_{BBI} measurements were calculated as the dihedral angle between planes of best fit for all nine atoms of each bibenzimidazole moiety system.
33 The ϕ torsion angles were measured as the dihedral angle between two planes: (1) the calculated plane of the six atoms in the ring directly attached to the BBI moiety at the 4- and 4′-positions; (2) the calculated plane of the nine-atom benzimidazole moiety to which the aryl substituent is attached.
34 Throughout this work, molecular structures that have been computed by DFT calculations will be referred to as 'computational structures' and molecular structures that have been determined by X-ray crystallography will be referred to as 'experimental structures'.
35 M. V. Baker, D. H. Brown, V. J. Hesler, B. W. Skelton and A. H. White, *Organometallics*, 2007, **26**, 250.
36 The atomic displacement ellipsoids are shown at 30% probability.
37 Average planes were calculated from the carbon and nitrogen atoms comprising the bibenzimidazole moieties in neighboring molecules. The mentioned angle refers to the angle between these two planes.
38 M. J. Frisch, G. W. Trucks, H. B. Schlegel, G. E. Scuseria, M. A. Robb, J. R. Cheeseman, V. G. Zakrzewski, J. A. J. Montgomery, R. E. Stratmann, J. C. Burant, S. Dapprich, J. M. Millam, A. D. Daniels, K. N. Kudin, M. C. Strain, O. Farkas, J. Tomasi, V. Barone, M. Cossi, R. Cammi, B. Mennucci, C. Pomelli, C. Adamo, S. Clifford, J. Ochterski, G. A. Petersson, P. Y. Ayala, Q. Cui, K. Morokuma, D. K. Malick, A. D. Rabuck, K. Raghavachari, J. B. Foresman, J. Cioslowski, J. V. Ortiz, B. B. Stefanov, G. Liu, A. Liashenko, P. Piskorz, I. Komaromi, R. Gomperts, R. L. Martin, D. J. Fox, T. Keith, M. A. Al-Laham, C. Y. Peng, A. Nanayakkara, C. Gonzalez, M. Challacombe, P. M. W. Gill, B. Johnson, W. Chen, M. W. Wong, J. L. Andres, C. Gonzalez, M. Head-Gordon, E. S. Replogle and J. A. Pople, *Gaussian 98*, Revision A.6, Pittsburgh PA, 1998.
39 M. W. Schmidt, K. K. Baldridge, J. A. Boatz, S. T. Elbert, M. S. Gordon, J. H. Jensen, S. Koseki, N. Matsunaga, K. A. Nguyen, S. Su, T. L. Windus and S. T. Elbert, *J. Comp. Chem.*, 1993, **14**, 1347.
40 A. D. Boese and J. M. L. Martin, *J. Chem. Phys.*, 2004, **121**, 3405.
41 T. H. Dunning, *J. Chem. Phys.*, 1989, **90**, 1007.
42 K. K. Baldridge and J. P. Greenberg, *J. Mol. Graphics*, 1995, **13**, 63.

